www.czasopisma.pan.pl PAN POLSKA AKADEMIA NAUK www.journals.pan.pl

*Metrol. Meas. Syst.*, Vol. 24 (2017), No. 1, pp. 153–160.

PAN POLSKA AKADEMIA NAUK

METROLOGY AND MEASUREMENT SYSTEMS

Index 330930, ISSN 0860-8229

*www.metrology.pg.gda.pl*

M&MS

# EXAMINATION OF SOL-GEL DERIVED HYDROXYAPATITE ENHANCED WITH SILVER NANOPARTICLES USING OCT AND RAMAN SPECTROSCOPY

**Maciej J. Głowacki[1,3], Marcin Gnyba[1], Paulina Strąkowska[1,3], Mateusz Gardas[2], Maciej Kraszewski[1], Michał Trojanowski[1], Marcin R. Strąkowski[1]**

*1) Gdańsk University of Technology, Faculty of Electronics, Telecommunications and Informatics, G. Narutowicza 11/12, 80-233 Gdańsk, Poland (margnyba@pg.gda.pl, pauanton@pg.gda.pl, mackrasz@student.pg.gda.pl, mictroja@pg.gda.pl*
*✉ marcin.strakowski@eti.pg.gda.pl, +48 58 347 1361)*
*2) Mateusz Gardas GAROCIN LABS, Świerkowa 4, 76-200 Słupsk, Poland (gardas.mateusz@gmail.com)*
*3) Gdańsk University of Technology, Faculty of Mechanical Engineering, G. Narutowicza 11/12, 80-233 Gdańsk, Poland (macglow1@student.pg.gda.pl)*

**Abstract**

*Hydroxyapatite* (HAp) has been attracting widespread interest in medical applications. In a form of coating, it enables to create a durable bond between an implant and surrounding bone tissues. With addition of silver nanoparticles HAp should also provide antibacterial activity. The aim of this research was to evaluate the composition of hydroxyapatite with silver nanoparticles in a non-destructive and non-contact way. For control measurements of HAp molecular composition and solvent evaporation efficiency the Raman spectroscopy has been chosen. In order to evaluate dispersion and concentration of the silver nanoparticles inside the hydroxyapatite matrix, the *optical coherence tomography* (OCT) has been used. Five samples were developed and examined – a reference sample of pure HAp sol and four samples of HAp colloids with different silver nanoparticle solution volume ratios. The Raman spectra for each solution have been obtained and analyzed. Furthermore, a transverse-sectional visualization of every sample has been created and examined by means of OCT.

Keywords: hydroxyapatite, sol-gel, nanoparticles, Raman spectroscopy, optical coherence tomography (OCT).



## 1. Introduction

Hydroxyapatite, $Ca_{10}(PO_4)_6(OH)_2$, commonly referred to as HAp, has been widely applied in bone surgery, implantation and dentistry. Biological (nonstoichiometric) hydroxyapatite is an inorganic compound naturally existing as a structural template for the mineral phase of vertebrate bones and teeth [1–2]. In elevated temperatures, when an appropriate metastable medium is applied, biological hydroxyapatite may also be obtained from marine invertebrate cartilage tissues [3]. Synthetic (stoichiometric) hydroxyapatite is a bio-ceramic material which can be manufactured using various methods, including wet precipitation, sol-gel processing, solid-state reactions, hydrothermal treatment or a flux method [4–10]. The sol-gel technique has several advantages over other methods suitable for preparing synthetic HAp. Firstly, it enables to replace high-temperature reactions of synthesis with low-temperature processes [11]. Secondly, it may be used for creating both fine powders and thin ceramic layers on complex surfaces [12]. Finally, due to a high fluidity of the sols, the samples prepared using the sol-gel processing are irradiated by light in their entire depth and therefore may be examined using optical measurement methods.

Due to its structural and compositional similarities with the natural bone, the artificial hydroxyapatite has the highest biocompatibility among currently known ceramic biomaterials [13–14]. It enables to create a durable biological bonding with surrounding bone tissues, causes osteoinductive activity and has no negative effects on human organism [4]. Unfortunately, HAp

Article history: received on Jul. 27, 2016; accepted on Sep. 24, 2016; available online on Mar. 10, 2017; DOI: 10.1515/mms-2017-0008.

does not exhibit antibacterial activity which would reduce the risk of infection during and after the insertion of an implant. To provide the hydroxyapatite with antiseptic properties, current research has been focused on combining the biomaterial with silver nanoparticles [15–16]. However, uniform distribution of the nanoparticles must be maintained in order to optimize material properties and to avoid disruption of the HAp structure. Poor mechanical properties of hydroxyapatite make it insufficient to be used as an implant experiencing severe stresses. Instead, HAp is often combined with metallic or polymer phases to create composites of satisfactory biomechanical performance.

The aim of this research was to develop a non-destructive optical measurement methodology for analysis of silver-hydroxyapatite nanocomposites prepared by the sol-gel technology. Regardless of the hydroxyapatite manufacturing process, the most common methods for its characterization are *scanning electron microscopy* (SEM), *X-ray diffraction* (XRD) and *Fourier-transform infrared* (FTIR) spectroscopy [5–10]. However, in order to examine an object supposed to work in the environment of human organism, it is reasonable to use techniques which enable to examine the material without changing its inner structure or causing damage. Conventional SEM is generally destructive due to special preparation methods which provide samples with electrical conductivity. Although FTIR spectroscopy and XRD are considered non-invasive, these techniques do not enable to visualize the internal structure of the analysed material. Therefore, in order to evaluate dispersion and concentration of silver nanoparticles inside the hydroxyapatite matrix, the *optical coherence tomography* (OCT) has been chosen. OCT has never been extensively used for HAp inspection and it is one of a few methods suitable for evaluation of nanocomposite materials which belong to the NDE/NDT group. For a qualitative analysis and control measurements of HAp the Raman spectroscopy has been selected.

## 2. Measurement techniques

The *optical coherence tomography* (OCT), which has been used in this study to examine distribution of silver nanoparticles inside the hydroxyapatite colloids, is a contact-free, non-invasive measurement technique widely known for its biomedical applications, especially in ophthalmology [17]. It has also proven to be useful in evaluation of technical objects and recent research results have shown its potential for nanocomposite material inspection [18–19]. OCT is based on low-coherence interferometry, therefore the light backscattered from particular points inside the evaluated material can be spatially detected and recorded. As a result, the depth-resolved reflectivity profiles of the sample, called A-scans, are obtained. Combining series of laterally *adjacent depth-scans* (A-scans) enables to generate cross-sectional images of the samples, known as B-scans. The OCT technique also enables to create 3D tomographic pictures. Although standard OCT systems deliver only intensity images, the backscattered signal provides more valuable data, *i.e.* spectral characteristic or polarization state of the light [20]. This additional information can be specified in the pictures by various image contrasting algorithms. Thereby, OCT may be extended to more advanced and sophisticated systems like *polarization-sensitive optical coherence tomography* (PS-OCT), which has been used in this study and is presented in Fig. 1 [20–21].

In the PS-OCT system, a light beam emitted by a broadband swept source is used for the measurements. The beam is linearly polarized before entering a *beam-splitter* (BS), which divides the incoming light into two sections - a sample arm containing the evaluated material and a reference arm, which includes a mirror. In the presented solution a Michelson interferometer is used. However, other types of two-beam interferometers, like Mach-Zehnder, can be successfully applied. Both arms of the interferometer contain *quarter-wave plates* (QWP), which let through all the incoming light, providing a stable polarization control, which

*Metrol. Meas. Syst.*, Vol. 24 (2017), No. 1, pp. 153–160.

is necessary for polarization sensitive analysis. The beam backscattered by the sample interferes with the light reflected from the reference arm at the *beam-splitter* (BS). Then, the *polarizing beam-splitter* (PBS) separates two orthogonal polarization states – horizontal and vertical – in order to provide detection of polarization diversity. Such a polarization-sensitive system delivers information about local changes of birefringence inside the sample structure.

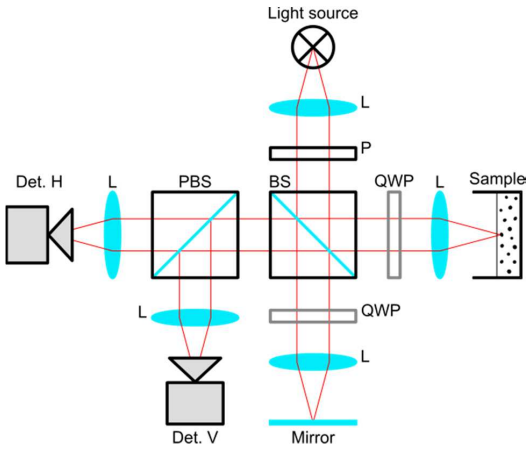


Fig. 1. A schematic diagram of a polarization-sensitive optical coherence tomography system. L – lens; P – polarizer; BS – *beam-splitter*; QWP – *quarter-wave plate*; PBS – *polarizing beam-splitter*; Det. – detector: V – vertical, H – horizontal.

A complementary method used to characterize the samples according to their optical properties is the Raman spectroscopy, which is a contact-free and non-invasive measurement technique based on inelastic scattering of light and is used for molecular identification of materials and their quantitative analysis [22–23]. The method, which is also complementary to IR spectroscopy, may be used to study solid, liquid and gaseous substances. The Raman spectroscopic system which has been used in this research is presented in Fig. 2.

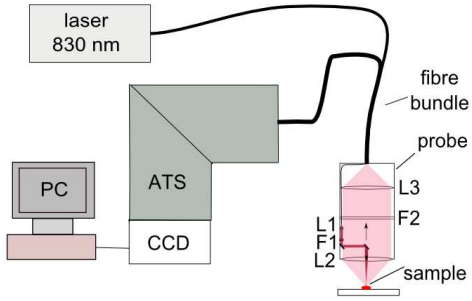


Fig. 2. A schematic diagram of the Raman spectroscopic system. L1, L2, L3 – lenses; F1 – laser line filter; F2 – low-pass filter; ATS – axial transmissive spectrograph; CCD – detector array; PC – computer.

The excitation wave signal from the laser can be delivered either through an open space or by a fiber optic probe. The laser line filter can be applied to ensure irradiation of samples by a single-frequency light. The collected scattering signal is transmitted to the spectrograph. When the Raman scattering occurs, the registered spectrum of light contains not only the

Rayleigh band with a frequency identical to that of the incident light but also symmetrically distant bands with a decreased and increased frequency, called Stokes and anti-Stokes lines, respectively. Their number and location depend on the internal structure of the samples and are unique for every material. Since the Raman scattering is very weak, there is a number of procedures taken to distinguish it from the predominant Rayleigh scattering, *e.g.* implementation of a low-pass or notch filter in the collection part. Moreover, the detector array is cooled to improve the signal-noise ratio. The Raman spectroscopy is non-destructive for the samples as long as the radiation intensity is controlled.

## 3. Experimental procedure

In the presented experiment, the silver-hydroxyapatite composite was synthesised by mixing an aqueous solution of silver nanoparticles with the hydroxyapatite colloid prepared using the sol-gel technique.

Calcium nitrate tetra-hydrate $Ca(NO_3)_2$ x $4H_2O$ and di-phosphorus pentoxide $P_2O_5$ were selected for the synthesis of HAp by the sol-gel method [24]. First, the di-phosphorus pentoxide was dissolved in ethyl alcohol, then the calcium nitrate tetra-hydrate was added to the solution to attain a Ca/P molar ratio of 1.67, which is the necessary condition for obtaining the synthetic hydroxyapatite. The transparent alcoholic solution of $P_2O_5$ turned into an opaque colloid after the addition of $Ca(NO_3)_2$ x $4H_2O$. A sample of pure HAp sol was prepared in a Petri dish and examined by the OCT method before the aging process. The Raman spectrum of the sample was also obtained and analysed.

In order to prepare the solution of silver nanoparticles, silver nitrate $AgNO_3$ and ascorbic acid were separately dissolved in deionized water containing polyvinyl alcohol PVA [25]. Then the aqueous solution of the ascorbic acid was added dropwise into the silver nitrate solution, which made the transparent liquid turn red. The resulting colloid, which darkened after being kept statically for 30 min, was added to the hydroxyapatite sol and stirred energetically. Four sols were prepared with different HAp sol to Ag nanoparticle solution volume ratios: 1/2, 1/1, 2/1, 3/1. A sample of each sol was prepared in the Petri dish and examined by means of OCT and the Raman spectroscopy. The diameter of silver nanoparticles was estimated to be below 300 nm.

The PS-OCT system used in this study has been developed at the Faculty of Electronics, Telecommunications and Informatics, Gdańsk University of Technology (Poland). The most important features of the OCT measurement system are summarized in Table 1.

Table 1. The PS-OCT system features.

| Item | Value |
|---|---|
| Light source type | 20 kHz swept source (SS) |
| Average output power | 10 mW |
| Central wavelength | 1320 nm |
| Wavelength range | 140 nm |
| Axial resolution | 12 μm |
| Lateral resolution | 15 μm |
| Frame rate | > 4 fps |
| Max. displaying imaging range / transverse imaging range | 7 mm / 10 mm |

The Raman spectroscopy was performed in a system based on a pre-commercial Ramstas spectrometer developed by the VTT – Technical Research Centre of Finland [26–28]. The characteristics of the Raman spectrometer system used in this research are presented in Table 2.

*Metrol. Meas. Syst.*, Vol. 24 (2017), No. 1, pp. 153–160.

Table 2. The Raman spectrometer characteristics.

| Item | Value |
|---|---|
| Light source type | Diode laser / CW mode, central wavelength 830 nm |
| Average power on sample | 100 mW |
| Spectrograph | Axial transmissive setup with holographic transmission grating |
| Detector | TE-cooled CCD array / 1024 rows |
| Spectral range | 200 – 2000 $cm^{-1}$ |
| Spectral resolution | 8 $cm^{-1}$ |
| Optical system | Fibre optics probe / working distance – 5 cm |

## 4. Results and discussion

The samples of hydroxyapatite placed in the Petri dishes were successfully measured using the polarization-sensitive optical coherence tomography. The obtained cross-sectional visualizations of every sample were examined. The resulting OCT images, which are presented in Fig. 3 with corresponding photographs of HAp samples, were well-detailed at any depth of the analyzed material.

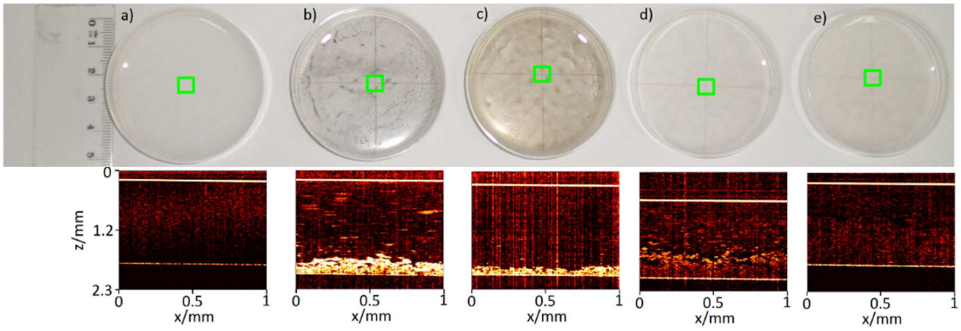


Fig. 3. The OCT images with corresponding photographs of HAp samples. Pure Hap (a); HAp/nanoparticles = 1/2 (b); HAp/nanoparticles = 1/1 (c); HAp/nanoparticles = 2/1 (d); HAp/nanoparticles = 3/1 (e). Green squares in the photographs indicate the OCT measurement areas (5.5 mm by 5.5 mm).

The OCT picture of pure HAp sol was used as a reference and every other sample was compared with it in order to evaluate the distribution of the silver nanoparticles inside the hydroxyapatite matrix. Although very small diameters of the nanoparticles place them below the resolution of the OCT system, and therefore their real dimensions could not be assessed in this measurement, still they are clearly visible in the pictures against the hydroxyapatite background and their degree of dispersion may be estimated. The sample with the lowest Ag content (the HAp sol to Ag nanoparticle solution volume ratio equal to 3/1) bears the closest resemblance to the reference sample of pure hydroxyapatite sol. This indicates that the nanoparticles are uniformly distributed inside the hydroxyapatite and the structure of the composite is quite homogeneous. In the case of samples with higher concentrations of silver, the nanoparticles have sunk to the bottom of Petri dishes and agglomerated into new phases, which are clearly visible in the images.

The Raman spectra of the sols obtained after mixing the components as well as the spectra of gels recorded after 24 hours of drying are shown in Fig. 4. Main bands at 880 $cm^{-1}$ and 1045 $cm^{-1}$ can be assigned to ethanol and ν(P-O) stretching mode of HAp, respectively.

Comparison of their intensity shows how efficiently ethanol evaporates during the drying process and how the structure of HAp is being created. In the case of spectra of the pure HAp sol and the sample with the lowest concentration of Ag nanoparticles the gelation was quite effective – the ethanol mostly evaporated during 24 hours and the (P-O)-based network of HAp was developing. This stays in a good agreement with the results obtained by OCT, which have shown that these samples present the best homogeneity and distribution of the nanoparticles. Contrary to them, samples with a higher Ag content still contained a larger content of non-vaporised ethanol and agglomerated Ag particles after 24 hours. It suggests that components of Ag colloids may interrupt ethanol evaporation and thus disturb uniform distribution of the silver nanoparticles. Moreover, these samples contain a huge amount of different unreacted particles and clusters which produces a stronger optical background.

The band assigned to P-O stretching is shifted towards higher wavenumbers in comparison to crystalline HAp (962 $cm^{-1}$) because materials were still in an elastic or liquid form (some ethanol remained inside) during the examination [29].

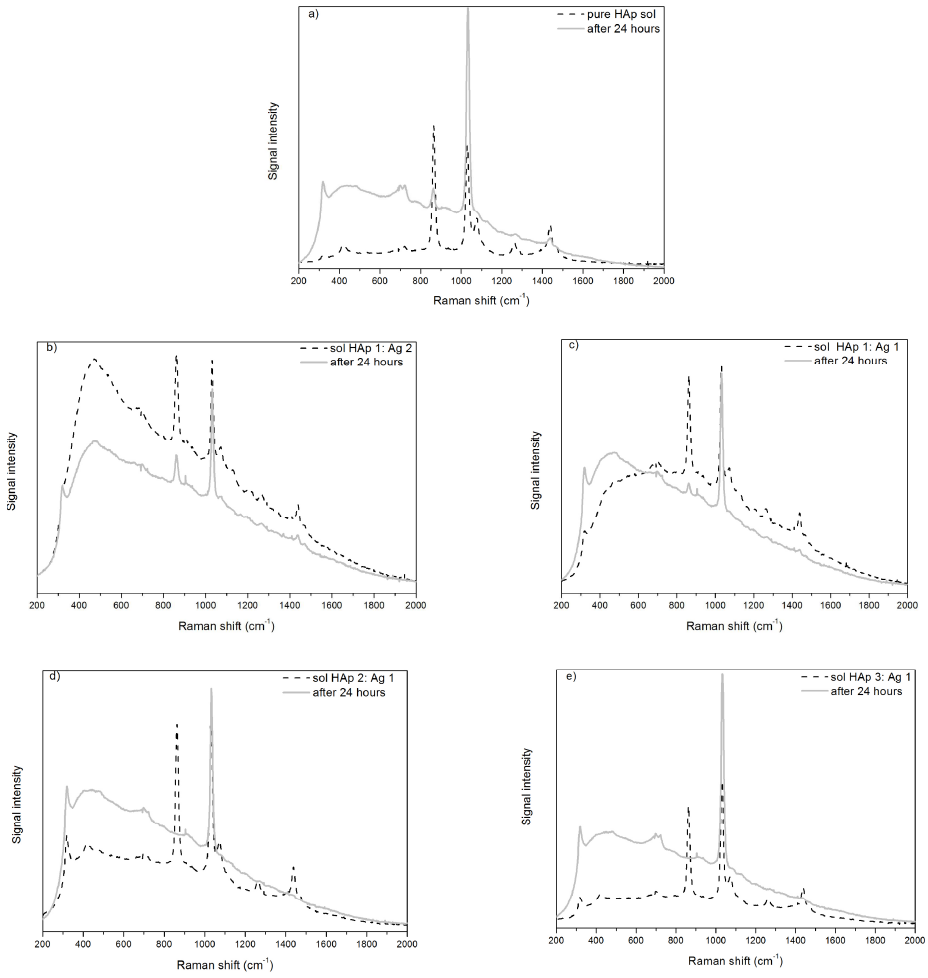


Fig. 4. The Raman spectra of HAp samples. Pure Hap (a); HAp/nanoparticles = 1/2 (b); HAp/nanoparticles = 1/1 (c); HAp/nanoparticles = 2/1 (d); HAp/nanoparticles = 3/1 (d). The spectra were recorded after synthesis of the sols and after 24 hours of drying.

*Metrol. Meas. Syst.*, Vol. 24 (2017), No. 1, pp. 153–160.

## 5. Conclusions

The results of presented research have confirmed a significant potential of simultaneous use of the optical coherence tomography and the Raman spectroscopy for non-destructive examination of nanocomposite materials based on HAp with Ag nanoparticles. Their use has enabled to select a sample with the best distribution of silver nanoparticles (in this particular case – the sample with the ratio of HAp/nanoparticles = 3/1) as well as to study processes which take place inside the material during the gelation and the lattice formation. The differences between light scattering determined by the OCT can be correlated with the differences of molecular composition of the material examined by the Raman spectroscopy. We correlated the better homogeneity of the sample and distribution of the Ag nanoparticles (OCT profile analysis) with the most efficient ethanol evaporation during the drying and with consequent better lattice formation (change of the intensity of respective Raman bands). Thus, our results have shown that the addition of the aqueous solution of the silver nanoparticles to the HAp sol may heavily disrupt the gelation and drying processes of the composite if the content of Ag solution is too high. The reason of such a disorder could be the fact that the two solutions were based on different solvents. Preparation of an aqueous HAp sol or an alcoholic solution of the silver nanoparticles could possibly solve the problem if introduction of a higher content to HAp is required.

## Acknowledgements

This research work has been supported by The National Centre for Research and Development (NCBiR), Poland, under the grant no. LIDER/32/205/L-3/11 and the DS program of Faculty of Electronics, Telecommunications and Informatics, Gdańsk University of Technology. The authors wish to thank the researchers from VTT – Technical Research Centre of Finland (Oulu) for providing a VTT Ramstas spectrometer.

## References

[1] Leventouri, Th. (2006). Synthetic and biological hydroxyapatites: Crystal structure questions. *Biomaterials*, 27, 3339–3342.

[2] Sadat-Shojai, M., Khorasani, M.T., Dinpanah-Khoshdargi, E., Jamshidi, A. (2013). Synthesis methods for nanosized hydroxyapatite with diverse structures. *Acta Biomaterialia*, 9, 7591–7621.

[3] Eilberg, R.G., Zuckerberg, D.A. (1975). Mineralization of Invertebrate Cartilage. *Calcif. Tiss. Res.*, 19, 85–90.

[4] Orlovskii, V.P., Komlev, V.S., Barinov, S.M. (2002). Hydroxyapatite and Hydroxyapatite-Based Ceramics. *Inorganic Materials*, 38(10), 973–984.

[5] Afshar, A., Ghorbani, M., Ehsani, N., Saeri, M.R., Sorrell, C.C. (2003). Some important factors in the wet precipitation process of hydroxyapatite. *Materials and Design*, 24, 197–202.

[6] Mobasherpour, I., Soulati Heshajin, M., Kazemzadeh, A., Zakeri, M. (2007). Synthesis of nanocrystalline hydroxyapatite by using precipitation method. *Journal of Alloys and Compounds*, 430, 330–333.

[7] Bogdanoviciene, I., Beganskiene, A., Tonsuaadu, K., Glaser, J., Meyer, H.J., Kareiva, A. (2006). Calcium hydroxyapatite, $Ca_{10}(PO_4)_6(OH)_2$ ceramics prepared by aqueous sol-gel processing. *Materials Research Bulletin*, 41, 1754–1762.

[8] Pramanik, S., Agarwal, A.K., Rai, K.N., Garg, A. (2007). Development of high strength hydroxyapatite by solid-state-sintering process. *Ceramics International*, 33, 419–426.

[9] Wang, Y., Zhang , S., Wei, K., Zhao, N., Chen, J., Wang, X. (2006). Hydrothermal synthesis of hydroxyapatite nanopowders using cationic surfactant as a template. *Materials Letters*, 60, 1484–1487.

[10] Teshima, K., Lee, S., Sakurai, M., Kameno, Y., Yubuta, K., Suzuki, T., Shishido, T., Endo, M., Oishi, S. (2009). Well-Formed One-Dimensional Hydroxyapatite Crystals Grown by an Environmentally Friendly Flux Method. *Crystals Growth & Design*, 9(6), 2937–2940.

[11] Mohseni, E., Zalnezhad, E., Bushroa, A.R. (2014). Comparative investigation on the adhesion of hydroxyapatite coating on Ti-6Al-4V implant: A review paper. *International Journal of Adhesion & Adhesives*, 48, 238–257.

[12] Brinker, C.J., Scherer, G.W. (1990). *Sol-Gel Science: The Physics and Chemistry of Sol-Gel Processing*. USA: Academic Press.

[13] Uklejewski, R., Winiecki, M., Mielniczuk, J., Rogala, P., Auguściński, A. (2008). The poroaccessibility parameters for three-dimensional characterization of orthopedic implants porous coatings. *Metrol. Meas. Syst.*, 15(2), 215–226.

[14] Batory, D., Gawronski, J., Kaczorowski, W., Niedzielska, A. (2012). C-HAp composite layers deposited onto AISI 316L austenitic steel. *Surface & Coatings Technology*, 206, 2110–2114.

[15] Andrade, F.A.C., de Oliveira Vercik, L.C., Monteiro, F.J., da Silva Rigo, E.C. (2016). Preparation, characterization and antibacterial properties of silver nanoparticles-hydroxyapatite composites by a simple and eco-friendly method. *Ceramics International*, 42, 2271–2280.

[16] Tian, B., Chen, W., Yu, D., Lei, Y., Ke, Q., Guo, Y., Zhu, Z. (2016). Fabrication of silver nanoparticle-doped hydroxyapatite coatings with oriented block arrays for enhancing bactericidal effect and osteoinductivity. *Journal of the mechanical behavior of biomedical materials*, 61, 345–359.

[17] Fercher, A.F., Drexler, W., Hitzenberger, C.K., Lasser, T. (2003). Optical coherence tomography - principles and applications. *Reports on Progress in Physics*, 66, 239–303.

[18] Strąkowski, M.R., Pluciński, J., Jędrzejewska-Szczerska, M., Hypszer, R., Maciejewski, M., Kosmowski, B.B. (2008). Polarization sensitive optical coherence tomography for technical materials investigation. *Sensors and Actuators A*, 142, 104–110.

[19] Trojanowski, M., Kraszewski, M., Strąkowski, M.R., Pluciński, J. (2015). Optical Coherence Tomography for nanoparticles quantitative characterization. *Proc. SPIE 9554, Nanoimaging and Nanospectroscopy III*, 95540I.

[20] Strąkowski, M.R., Pluciński, J., Kosmowski, B.B. (2011). Polarization Sensitive Optical Coherence Tomography with Spectroscopic Analysis. *Acta Physica Polonica A*, 120(4), 785–788.

[21] Pircher, M., Hitzenberger, C.K., Schmidt-Erfurth, U. (2011). Polarization sensitive optical coherence tomography in the human eye. *Progress in Retinal and Eye Research*, 30, 431–451.

[22] Kwiatkowski, A., Gnyba, M., Smulko, J., Wierzba, P. (2010). Algorithms of chemicals detection using Raman spectra. *Metrol. Meas. Syst.*, 17(4), 549–560.

[23] Ferraro, J.R., Nakamoto, K., Brown, C.W. (2003). *Introductory Raman Spectroscopy*. Elsevier.

[24] Kim, I., Kumta, P.N. (2004). Sol-gel synthesis and characterization of nanostructured hydroxyapatite powder. *Materials Science and Engineering B*, 111, 232–236.

[25] Zielinska, A., Skwarek, E., Zaleska, A., Gazda, M., Hupka, J. (2009). Preparation of silver nanoparticles with controlled particle size. *Procedia Chemistry*, 1, 1560–1566.

[26] Niemelä, P., Suhonen, J. (2001). Rugged Fiber-Optic Raman Probe for Process Monitoring Applications. *Applied Spectroscopy*, 55(10), 1337–1340.

[27] Gnyba, M., Keränen, M., Maaninen, A., Suhonen, J., Jędrzejewska-Szczerska, M., Kosmowski, B.B., Wierzba, P. (2005). Raman system for on-line monitoring and optimization of hybrid polymer gelation. *Opto-Electronics Review*, 13(1), 9–17.

[28] Gnyba, M., Keraenen, M. (2003). Optical investigation of molecular structure of sophisticated materials for photonics. *Proc. SPIE*, 5125, 339–344.

[29] Koutsopoulos, S. (2002). Synthesis and characterization of hydroxyapatite crystals: A review study on the analytical methods. *Journal of Biomedical Materials Research*, 62(4), 600–612.